Metal–Metal Interactions

DOI: 10.1002/ange.201405240

First Stabilization of 14-Electron Rhodium(I) Complexes by Hemichelation**

Christophe Werlé, Corinne Bailly, Lydia Karmazin-Brelot, Xavier-Frédéric Le Goff, Michel Pfeffer, and Jean-Pierre Djukic**

Abstract: *Hemichelation is emerging as a new mode of coordination where non-covalent interactions crucially contribute to the cohesion of electron-unsaturated organometallic complexes. This study discloses an unprecedented demonstration of this concept to a Group 9 metal, that is, Rh^I. The syntheses of new 14-electron Rh^I complexes were achieved by choosing the anti-[(η^6:η^6-fluorenyl){$Cr(CO)_3$}$_2$] anion as the ambiphilic hemichelating ligand, which was treated with [{$Rh(nbd)Cl$}$_2$] (nbd = norbornadiene) and [{$Rh(CO)_2Cl$}$_2$]. The new T-shaped Rh^I hemichelates were characterized by analytical and structural methods. Investigations using the methods of the DFT and electron-density topology analysis (NCI region analysis, QTAIM theory) confirmed the closed-shell, non-covalent and attractive characters of the interaction between the Rh^I center and the proximal $Cr(CO)_3$ moiety. This study shows that, by appropriate tuning of the electronic properties of the ambiphilic ligand, truly coordination-unsaturated Rh^I complexes can be synthesized in a manageable form.*

In transition-metal chemistry, coordinatively unsaturated species are often assumed to be central in a number of chemical transformations.[1] A host of reports have outlined that such potentially reactive species can be stabilized by weak intramolecular agostic C–H···M interactions,[1e,2] which can be challenged by solvent coordination.[3] The problems of reactivity can be circumvented by producing steric cluttering around the metal center that may prevent access of the free coordination site to any occasional ligand, as shown by Figueroa et al.[4] and Chaplin.[5] A number of stable and persistent valence-unsaturated organometallic complexes have been synthesized,[6] where the interplay between peculiar molecular conformations and compactness and van der Waals interactions, such as the dispersion force,[7] appeared to play a key role. Recent studies[8] have shown that non-covalent interactions are essential in the stabilization of electronically unsaturated metal centers in isolable, conformationally flexible species. In this respect, the concept of hemichelation[8a] introduces a new approach in coordination chemistry that is based on the central role of non-covalent attractive interactions in the stabilization of apparently unviable species and relativizes the importance of the empirical Langmuir–Sidgwick so-called 18-electron rule in transition-metal chemistry. Hemichelation can be achieved with ambiphilic anionic ligands, such as the [(η^6-indenyl)$Cr(CO)_3$]$^-$ ion prepared from **1a** by benzylic deprotonation, which can bind Pd^{II}[8] (Scheme 1) and Pt^{II}[8a] centers by

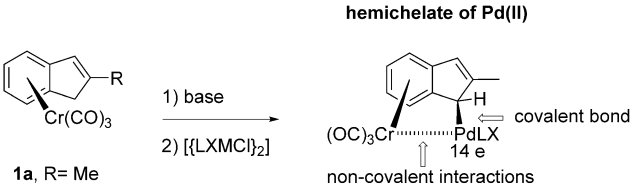

Scheme 1. Hemichelation[8a] is the preferred bonding mode for Group 10 metals, such as Pd^{II} and Pt^{II}, with the ambiphilic anion derived from **1a**.

means of 1) a covalent bond to the benzylic position and 2) non-covalent interactions of dominating Coulombic character with the proximal $Cr(CO)_3$ moiety, leading to persistent and manageable 14 valence electron complexes of Group 10 metals. Herein we disclose the first extension of the concept of hemichelation[8a] to Rh^I centers with an hemichelating ambiphilic anionic ligand of electronic properties chosen so as to promote structural cohesion by non-covalent intermetallic interactions. Unprecedented cases of 14 electron, T-shaped Rh^I complexes[1g–k,2d] stabilized by hemichelation are reported and the underlying issues of bonding analyzed by state-of-the-art methods using dispersion-accounting density functional theory[9] (DFT-D).

From the experience acquired with the stabilization of Pd^{II} and Pt^{II} hemichelates,[8a] the anion derived from **1a** looked promising because the slight steric hindrance of the methyl group at the 2 position could purportedly orient the coordination of the Rh^I center in a *syn*-facial manner so as to give exclusively the formation of a η^1-bonded Rh hemichelate. In fact the reaction of the anion of **1a** with [{Rh(cod)Cl}$_2$],[10] [{Rh(nbd)Cl}$_2$],[11] and [{$Rh(CO)_2Cl$}$_2$][12]

[*] C. Werlé, C. Bailly, Dr. L. Karmazin-Brelot, Dr. M. Pfeffer, Dr. J.-P. Djukic
Institut de Chimie de Strasbourg, UMR 7177 CNRS
Université de Strasbourg
4 rue Blaise Pascal, 67070 Strasbourg Cedex (France)
E-mail: pfeffer@unistra.fr
djukic@unistra.fr
Homepage: http://lcsom.u-strasbg.fr
X.-F. Le Goff
Département de Chimie, Ecole Polytechnique, Palaiseau cedex (France)

[**] This work was supported by the National Research Agency (ANR project WEAKINTERMET-2DA), the Laboratory of Excellence "Chemistry of Complex Systems" and the Centre National de la Recherche Scientifique.

Supporting information for this article is available on the WWW under http://dx.doi.org/10.1002/anie.201405240.

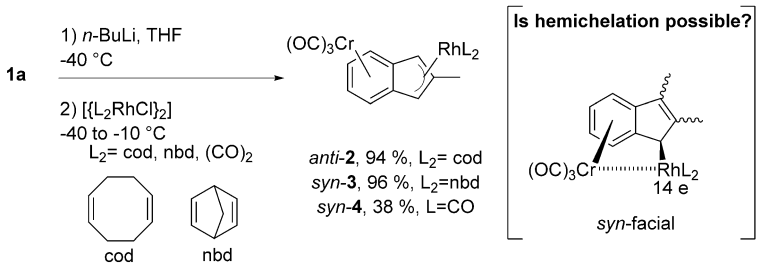

Figure 1. The sequential reaction of **1a** with *n*-BuLi and $[\{L_2RhCl\}_2]$ dimers operates different facial selection depending on the steric requirements of L_2 ligands. According to Ceccon et al.[13b–e] the η^3 (*syn*-facial) or η^2:η^3 (*anti*-facial) are the preferred coordination modes of the Rh^IL_2 moiety to the indenyl ligand with a net thermodynamic drive for the dispersion-favored *syn*-facial arrangement according to Grimme et al.[14] Hence, how to make hemichelation possible?

(Figure 1) produced products akin to those already reported by Ceccon et al.[13] These new compounds, namely *anti*-**2**, *syn*-**3**, and *syn*-**4** (Figure 1) were isolated in pure form and structurally characterized by X-ray diffraction analysis. In *anti*-**2**, the bulky [Rh(cod)] fragment was found to bind in an *anti*-facial manner, whereas in *syn*-**3** and *syn*-**4** the respective [Rh(nbd)] and $[Rh(CO)_2]$ fragments where found to bind in a *syn*-facial manner (Figure 2). In *syn*-**3** and *syn*-**4** the Rh^I center (16 electrons) was found to bind in a η^3 mode to the 1,2,3 positions of the indenyl, quite not in the expected hemichelation η^1 bonding mode. In *anti*-**2** the Rh^I center (formally 18 electrons) was clearly engaged in a dissymmetric η^2:η^3 coordination mode with the five-membered ring (Figure 2). Ceccon and co-workers[13b–e] demonstrated indeed that, with a similar anion prepared from $[(\eta^6\text{-indene})Cr(CO)_3]$, reactions of $[\{RhL_2Cl\}_2]$ complexes would lead under thermodynamic control[13d] to the *syn*-facial η^3 coordination of the Rh center to the five-membered ring when the L_2 moiety operates limited steric hindrance.

This thermodynamic preference for the *syn*-facial product over the *anti*-facial one was recently rationalized[14] by Grimme et al. as a direct consequence of the attractive stabilizing and driving effects of electron correlation and dispersion force acting between the $Cr(CO)_3$ moiety and the η^3-bonded RhL_2 fragment.

Keeping in perspective the synthesis of Rh^I 14-electron hemichelates, it became clear that the electronic properties of the ambiphilic ligand had to be tuned to preclude completely the possibility of a η^3 coordination of the Rh center, but without compromising the *syn*-facial selectivity of the binding of the $[RhL_2]$ fragment. In other words, the structure of the ambiphilic ligand had to be changed so as to leave no other choice to the Rh^I center but to form a hemichelate. It was found that the most promising way to achieve this goal was by using an analogue of **1a** with a fluorenyl motive instead of the indenyl. As shown in Figure 3, analysis of the partial natural charges (natural population analysis; NPA)[15] of singlet ground state geometries of **1a**, **1b**, and *anti*-**1c** (throughout this computed models were optimized at the ZORA-TPSS[16]-D3(BJ)[9a]/all electron TZP level) indicates that the strongest depletion of charge density at the aromatic carbon atoms at the 2,3

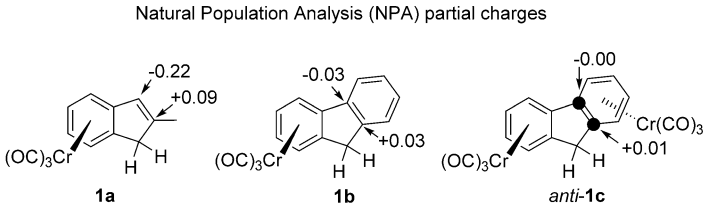

Figure 3. Natural partial charges (NPA) at C2 and C3 positions in **1a** and **1b–c** computed from gas-phase singlet ground state geometries optimized at the ZORA-TPSS-D3(BJ)/all electron TZP level.

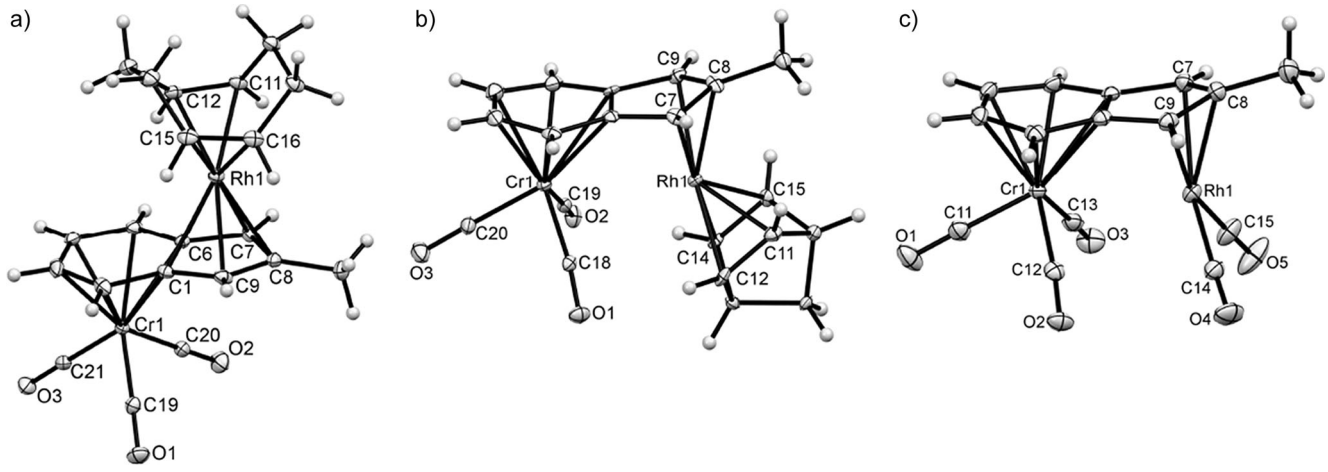

Figure 2. ORTEP diagrams of the structures of compounds a) *anti*-**2**, b) *syn*-**3**, and c) *syn*-**4**, thermal ellipsoids set at 30% probability. Selected interatomic distances [Å] and angles [°] for a) *anti*-**2**: Rh1-C7 2.248(3), Rh1-C8 2.276(3), Rh1-C9 2.223(3), Cr1-C20 1.842(3), Cr1-C19 1.839(3); C19-Cr1-C20 87.26(14). For b) *syn*-**3**: Rh1-C7 2.224(6), Rh1-C8 2.190(6), Rh1-C9 2.248(7), Rh1-C11 2.105(7), Rh1-C12 2.155(7), Rh1-C15 2.125(6), Rh1-C14 2.172(6), Rh1···Cr1 3.156(6), Cr1-C20 1.819(7), Cr1-C19 1.839(7), Cr1-C18 1.855(6); C19-Cr1-C18 94.0(3). For c) *syn*-**4**: Rh1-C7 2.232(3), Rh1-C8 2.193(3), Rh1-C9 2.204(3), Rh1-C15 1.878(4), Rh1-C14 1.877(3), Rh1···Cr1 3.0674(5), Cr1-C13 1.854(3), Cr1-C12 1.853(3), Cr1-C11 1.812(3); C12-Cr1-C13 94.01(13), C14-Rh1-C15 92.21(15).

positions occurs with *anti*-**1c**. This depletion is a necessary condition to prevent an η^3 bonding mode to the Rh^I center, which therefore made *anti*-**1c** a reasonable candidate for attempting the synthesis of Rh^I hemichelates.

Complex *anti*-**1c**[17] was readily synthesized and isolated in 50% yield as the major product of the thermolysis of excess $[Cr(CO)_6]$ in the presence of fluorene and catalytic amounts of naphthalene in a refluxing 1:10 mixture of THF and di-*n*-butylether for around 6 days. Complex *anti*-**1c** was subsequently deprotonated[17] by reaction with *n*-BuLi at −40 °C and treated in two separate experiments with $[\{Rh(nbd)Cl\}_2]$ and $[\{Rh(CO)_2Cl\}_2]$ yielding single products, respectively, *syn*-**5** and *syn*-**6** (Figure 4). These two complexes proved to be

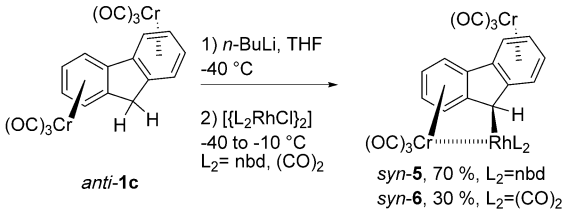

Figure 4. Formation of hemichelates *syn*-**5** and *syn*-**6** by sequential deprotonation and metalation of the benzylic position of *anti*-**1c**.

unstable in solution at room temperature and to generally decompose into *anti*-**1c** and untraceable material. Isolation of the products was however possible by repeated recrystallizations at temperatures around −20 °C. Analyses by ^{13}C and ^1H NMR spectroscopy were therefore carried out below −20 °C in dry [D_8]toluene or [D]chloroform. The most notable ^{13}C NMR spectral feature common to *syn*-**5** and *syn*-**6** is the signature of the $Cr(CO)_3$ moiety proximal to Rh, which appears as a three broad signals of low intensity at approximately $\delta = 234.4$, 233.7, and 227.1 ppm.

In the case of *syn*-**6**, the $Rh(CO)_2$ moiety resonates as two distinct signals in the ^{13}C NMR spectrum, that is, a broad signal at $\delta =$ 182.6 ppm and a well-resolved doublet at $\delta =$ 191.6 ppm displaying a Rh–C_{CO} coupling constant of 69 Hz, which suggests that the $Rh(CO)_2$ moiety undergoes a fast rotational exchange around the Rh–$C_{benzylic}$ axis producing a time-averaged signal for the equatorial Rh-bound carbonyl ligand and a fine doublet for the axial Rh-bound CO ligand. Quite notable is also the ^{13}C NMR response of the benzylic CH fragment at $\delta = 26.3$ and 37.3 ppm for *syn*-**5** and *syn*-**6**, respectively: with both complexes, this signal is a doublet of scalar ^1H-^{103}Rh coupling constant amounting to approximately 1.5 Hz. The ^{13}C signal arising from this fragment with *syn*-**5** is a resolved doublet ($J_{H\text{-}Rh} = 15$ Hz) whereas with *syn*-**6** it is a broad and barely resolved doublet ($J_{H\text{-}Rh} = 6.9$ Hz), which supports the assumption of a conformational exchange of the $Rh(CO)_2$ moiety.

The structures of *syn*-**5** and *syn*-**6** (Figure 5) were resolved by X-ray diffraction analyses of crystals grown at −20 °C. In both cases, the RhL_2 fragment is η^1-bonded to the fluorenyl ligand at the benzylic carbon and the Rh atom is about 2.81 Å from the Cr center, that is, about the sum of van der Waals radii for the two metals.[18] In both cases, the $Cr(CO)_3$ group proximal to the RhL_2 moiety is only slightly distorted and adopts an *anti*-eclipsed conformation with respect to the benzylic position materialized by atom C13 (Figure 5).

Theoretical analysis of the Rh–$C_{benzylic}$ bond in models *syn*-**5** (Wiberg bond index (wbi) 0.37) and *syn*-**6** (wbi = 0.31) by the natural bond orbital (NBO) method[15] points to a coordinative σ bond wherein the partially negatively charged carbon atom (NPA $qC_{benzylic} \approx$-0.42) contributes by an orbital hybridization of marked p character (sp^8 in *syn*-**5** and syn-**6**, bonding orbital population approximately 1.7 electron) to the bond with Rh. Further analysis of *syn*-**5** and *syn*-**6** by Yang's treatment of the reduced density gradient, which reveals the spatial distribution of intimate non-covalent interactions (NCI),[19] indicates that the RhL_2 fragments interact with the neighboring $Cr(CO)_3$ moiety through attractive non-covalent interactions (red isosurfaces, Figure 6c,d). Analysis of the topology of the electron density by the theory of atoms in molecules (AIM)[20] reveals a bond critical point (3,-1) (BCP) for the Cr–Rh segment in *syn*-**6** of low electron density ρ amounting to 0.0403 a.u. (Table 1). In the case of *syn*-**5**, no BCP is found in the Cr–Rh segment (Table 1). It is generally considered that ρ values of a magnitude of 10^{-2} a.u. and negative values of the Laplacian $-{}^1/_4 \nabla^2\rho$ at a BCP are associated with closed-shell interactions, that is, van der Waals interactions.[20b] This is well exemplified by the ρ values at BCP for models *syn*-**3** and *syn*-**4** (Table 1) for which it is evident, from NCI plots (Figure 6a,b), that the metal–metal interaction is non-covalently attractive.[19b]

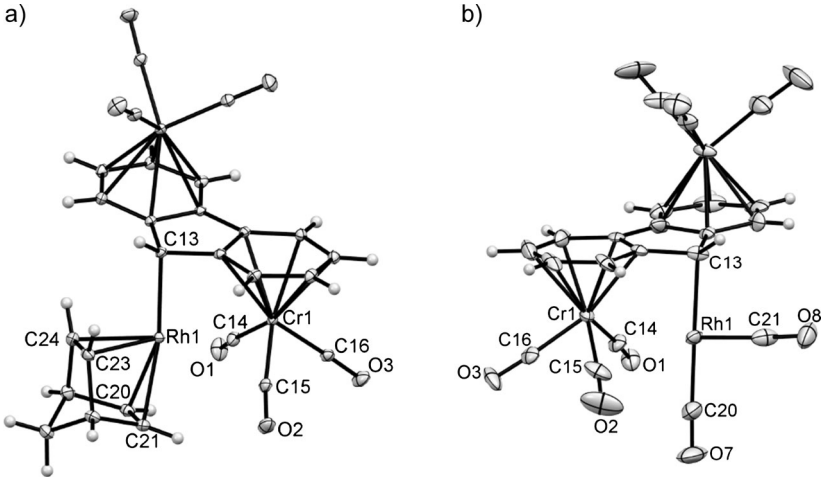

Figure 5. ORTEP diagrams of the structures of hemichelates a) *syn*-**5** and b) *syn*-**6**, thermal ellipsoids set at 30% probability. Selected interatomic distances [Å] and angles [°] for a) *syn*-**5**: Rh1···Cr1 2.8237(2), C13-Rh1 2.1724(12), C20-C21 1.382(2), C23-C24 1.405(2), Cr-C14 1.8708(15), Cr-C15 1.8492(15), Cr-C16 1.8382(14), Rh1-C21 2.1948(13), Rh1-C20 2.1980(14), Rh1-C23 2.1128(14), Rh1-C24 2.1262(15); C14-Cr1-C15 98.24(7). For b) *syn*-**6**: Cr1···Rh1 2.802(4), C13-Rh1 2.16(2), Rh1-C21 1.86(3), Rh1-C20 1.88(3), C21-O8 1.13(4), C20-O7 1.13(4); C15-Cr1-C14 99.8(14).

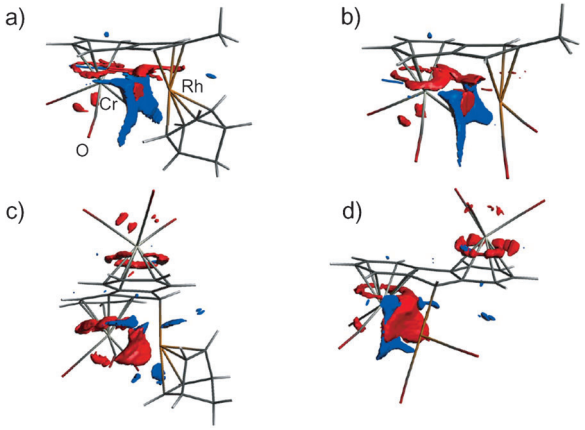

Figure 6. Plots of non-covalent interaction (NCI) regions shown as reduced density gradient isosurfaces (cut-off value $s = 0.02$ a.u., $\rho = 0.05$ a.u.) colored according to the sign of the signed density $\lambda_2\rho$ for gas-phase relaxed singlet ground state models of Rh-containing complexes *syn*-**3**, *syn*-**4**, *syn*-**5**, and *syn*-**6**; red: negatively (attractive) and blue: positively (repulsive) signed terms.

Table 1: Selected structural and electronic information on gas-phase singlet ground state model structures of *syn*-**3**, -**4**, -**5**, and -**6**.

Parameters	*syn*-**3**	*syn*-**4**	*syn*-**5**	*syn*-**6**
d(Cr–Rh) (Å)	3.135	3.062	2.679	2.776
d(Rh–$C_{benzylic}$) (Å)	2.254[a]	2.231[a]	2.203	2.213
q(Cr)[b]	−0.80	−0.82	−0.80	−0.81
q(Rh)[b]	+0.53	+0.22	+0.44	+0.10
$\Delta\Delta E_{int}$(Cr(CO)$_3$···fragment)[c] (kcal mol^{-1})	−12.5	−6.0	−40.0	−37.9
ρ (3,-1; Cr–Rh) (a.u.)[d]	0.0214	0.0245	no BCP	0.0403
$-^1/_4\nabla^2\rho$ (3, −1; Cr–Rh) (a.u.)[d]	−0.0083	−0.0080	–	−0.0113
wbi(Cr–Rh)[e]	0.06	0.05	0.18	0.14

[a] averaged value. [b] from natural population analysis. [c] ΔE_{int}(Cr(CO)$_3$···fragment) for **1a** = −73.9 kcal mol^{-1}, ΔE_{int}(Cr(CO)$_3$···fragment) for **1c** = −72.1 kcal mol^{-1}; $\Delta\Delta E_{int}$(Cr(CO)$_3$···fragment)$_i$ = ΔE_{int}(Cr(CO)$_3$···fragment)$_i$ − ΔE_{int}(Cr(CO)$_3$···fragment)$_{ref}$. [d] the density ρ and the Laplacian of the density $\nabla^2\rho$ at BCP (3,-1) were computed with Bader's AIM method. [e] Wiberg's bond index.[21]

ETS-NOCV[22] analyses of the interaction of the prepared Cr(CO)$_3$ moiety with the remaining organorhodium entity in *syn*-**5** and *syn*-**6** rationalize the slight shift of approximately 9 cm^{-1} to higher frequencies of the IR CO stretching bands of the Cr(CO)$_3$ moiety in *syn*-**5** and *syn*-**6** compared to reference compound **1c**. Deformation density plot $\Delta\rho_1$ (Figure 7) indicates that in *syn*-**6** a portion of electron density is transferred from the Cr(CO)$_3$ fragment towards the intermetallic space and the Rh center with minor back-donation contribution from the Rh to the Cr center ($\Delta\rho_3$, Figure 7). This suggests that in the Rh-hemichelates reported herein some Cr→Rh donor–acceptor character residually exists, which slightly dominates the Rh→Cr back-donation. Natural partial charges[15] (NPA) at Rh and Cr outline the key role of the attractive Coulombic contribution to the stabilization of *syn*-**5** and *syn*-**6**, which also receives the support of favorable dispersion and orbital interaction energy terms in the compensation of Pauli repulsion. This is illustrated by a larger difference in interfragment interaction energy $\Delta\Delta E_{int}$ for *syn*-**5** and *syn*-**6** (**1c** is the reference) than for *syn*-**3** and *syn*-**4** (**1a** is the reference); $\Delta\Delta E_{int}$ is used in this case as a measure of the energetic structural cohesion of a given complex with respect to a structure-related reference for a pertinent fragment interaction scheme (in this case the (CO)$_3$Cr-to-arene bonding).[8a] The attractive Coulombic contribution to the (CO)$_3$Cr-to-arene bonding is evaluated to be stronger by one order of magnitude in the Rh hemichelates than in Ceccon's type of *syn*-facial bimetallic compounds *syn*-**3** and *syn*-**4**.

In summary, this study demonstrates that the concept of hemichelation applies to Rh^I complexes. The use of the ambiphilic fluorenyl anion enables the formation of relatively persistent hemichelates wherein the Rh atom holds formally an unsaturated 14 valence-electron shell with a loose but stabilizing non-covalent interaction at its fourth coordination site. Apart from validating the whole concept of hemichelation, this study shows the multifaceted role played by the arene-bound Cr(CO)$_3$ moiety in the cohesion of unusual organometallic architectures. These results also broaden the potential of hemichelation, which offers a new alternative for the production of coordinatively unsaturated and potentially reactive metal centers.

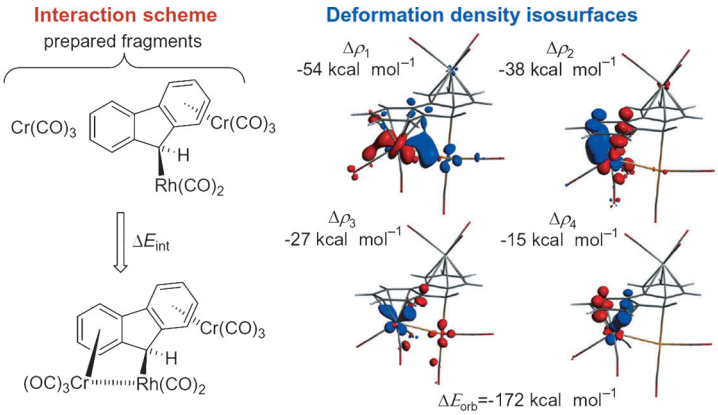

Figure 7. ETS-NOCV[22] deformation densities $\Delta\rho$ and the associated orbital interaction energies for the interaction of prepared Cr(CO)$_3$ with the Rh-fluorenyl fragment of *syn*-**6**. Isosurfaces show regions where charge density depletion (red) and build up (blue) occur upon interaction of the two fragments: electron-density transfer operates from red areas to blue ones upon bonding. Density isosurface contour = 0.005 e bohr^{-3}.

Experimental Section

General procedure for *syn*-**5** and *syn*-**6**: A solution of *anti*-[(η^6;η^6-fluorene){Cr(CO)$_3$}$_2$] (*anti*-**1c**) in dry and degassed THF (10 mL) was treated with 1 equiv of *n*-BuLi at −40 °C under argon atmosphere. The resulting solution of the fluorenylic anion was transferred after 45 min by cannula into a THF solution (5 mL) of 1 equiv of the corresponding rhodium(I) μ-chlorido bridged dimer complex at

−40 °C. The resulting mixture was stirred for 2 h during which the temperature was slowly raised to −20 °C. The solvent was then removed under reduced pressure and the residue extracted with cold diethyl ether. After filtration through dry Celite the solvent was removed under reduced pressure and the residue, contaminated with **1c**, was recrystallized several times from mixtures of diethyl ether and pentane until dark red crystals devoid of traces of yellow **1c** were obtained. Specific procedure details and analytical data are available in the Supporting Information.

CCDC 999054, 999055, 999056, 999057, 999058, and 999059 contain the supplementary crystallographic data for this paper. These data can be obtained free of charge from The Cambridge Crystallographic Data Centre via www.ccdc.cam.ac.uk/data_request/cif.

Received: May 13, 2014
Revised: June 4, 2014
Published online: July 17, 2014

Keywords: chromium · coordination modes · hemichelation · metal–metal interactions · rhodium

[1] a) J. A. Casares, P. Espinet, G. Salas, *Chem. Eur. J.* **2002**, *8*, 4843 – 4853; b) M. A. Ortuno, S. Conejero, A. Lledós, *Beilstein J. Org. Chem.* **2013**, *9*, 1352 – 1382; c) Y. W. Yared, S. L. Miles, R. Bau, C. A. Reed, *J. Am. Chem. Soc.* **1977**, *99*, 7076 – 7078; d) J. P. Stambuli, C. D. Incarvito, M. Bühl, J. F. Hartwig, *J. Am. Chem. Soc.* **2004**, *126*, 1184 – 1194; e) J. P. Stambuli, Z. Weng, C. D. Incarvito, J. F. Hartwig, *Angew. Chem.* **2007**, *119*, 7818 – 7821; *Angew. Chem. Int. Ed.* **2007**, *46*, 7674 – 7677; f) Y. Feng, C. Wang, H. Fan, *J. Organomet. Chem.* **2011**, *696*, 4064 – 4069; g) N. Chandrashekhar, V. Gayathri, N. M. N. Gowda, *Polyhedron* **2010**, *29*, 288 – 295; h) A. Vigalok, Y. Ben-David, D. Milstein, *Organometallics* **1996**, *15*, 1839 – 1844; i) G. Giordano, E. Rotondo, *Polyhedron* **1994**, *13*, 2507 – 2511; j) Y. Masashi, R. Noyori, *Organometallics* **1992**, *11*, 3167 – 3169; k) A. A. H. Van der Zeijden, G. Van Koten, R. A. Nordemann, B. Kojic-Prodic, A. L. Spek, *Organometallics* **1988**, *7*, 1957 – 1966; l) R. A. Gossage, H. A. Jenkins, N. D. Jones, R. C. Jones, B. F. Yates, *Dalton Trans.* **2008**, 3115 – 3122; m) D. V. Yandulov, N. T. Tran, *J. Am. Chem. Soc.* **2007**, *129*, 1342 – 1358; n) V. P. Ananikov, D. G. Musaev, K. Morokuma, *Eur. J. Inorg. Chem.* **2007**, 5390 – 5399; o) C. Amatore, A. Bucaille, A. Fuxa, A. Jutand, G. Meyer, A. N. Ntepe, *Chem. Eur. J.* **2001**, *7*, 2134 – 2142; p) K. Tatsumi, R. Hoffmann, A. Yamamoto, J. K. Stille, *Bull. Chem. Soc. Jpn.* **1981**, *54*, 1857 – 1867.

[2] a) H. Urtel, C. Meier, F. Eisenträger, F. Rominger, J. P. Joschek, P. Hofmann, *Angew. Chem.* **2001**, *113*, 803 – 806; *Angew. Chem. Int. Ed.* **2001**, *40*, 781 – 784; b) M. D. Walter, P. S. White, M. Brookhart, *New J. Chem.* **2013**, *37*, 1128 – 1133; c) O. Rivada-Wheelaghan, M. A. Ortuno, J. Diez, A. Lledos, S. Conejero, *Angew. Chem.* **2012**, *124*, 4002 – 4005; *Angew. Chem. Int. Ed.* **2012**, *51*, 3936 – 3939; d) M. Hasegawa, Y. Segawa, M. Yamashita, K. Nozaki, *Angew. Chem.* **2012**, *124*, 7062 – 7066; *Angew. Chem. Int. Ed.* **2012**, *51*, 6956 – 6960.

[3] M. A. Ortuno, P. Vidossich, G. Ujaque, S. Conejero, A. Lledós, *Dalton Trans.* **2013**, *42*, 12165 – 12172.

[4] B. M. Emerich, C. E. Moore, B. J. Fox, A. L. Rheingold, J. S. Figueroa, *Organometallics* **2011**, *30*, 2598 – 2608.

[5] A. B. Chaplin, *Organometallics* **2014**, *33*, 624 – 626.

[6] a) I. Hyla-Kryspin, S. Grimme, J.-P. Djukic, *Organometallics* **2009**, *28*, 1001 – 1013; b) C. Werlé, X.-F. Le Goff, J.-P. Djukic, *J. Organomet. Chem.* **2014**, *751*, 754 – 759; c) J.-P. Djukic, C. Michon, A. Maisse-Francois, R. Allagapen, M. Pfeffer, K. H. Dotz, A. De Cian, J. Fischer, *Chem. Eur. J.* **2000**, *6*, 1064 – 1077; d) S. Büschel, A.-K. Jungton, T. Bannenberg, S. Randoll, C. G. Hirb, P. G. Jones, M. Tamm, *Chem. Eur. J.* **2009**, *15*, 2176 – 2184.

[7] a) S. Grimme, J.-P. Djukic, *Inorg. Chem.* **2010**, *49*, 2911 – 2919; b) S. Grimme, J.-P. Djukic, *Inorg. Chem.* **2011**, *50*, 2619 – 2628.

[8] a) C. Werlé, C. Bailly, L. Karmazin-Brelot, X.-F. Le Goff, L. Ricard, J.-P. Djukic, *J. Am. Chem. Soc.* **2013**, *135*, 17839 – 17852; b) C. Werlé, M. Hamdaoui, C. Bailly, X.-F. Le Goff, L. Brelot, J.-P. Djukic, *J. Am. Chem. Soc.* **2013**, *135*, 1715 – 1718.

[9] a) S. Grimme, S. Ehrlich, L. Goerigk, *J. Comput. Chem.* **2011**, *32*, 1456 – 1465; b) S. Grimme, R. Huenerbein, S. Ehrlich, *ChemPhysChem* **2011**, *12*, 1258 – 1261; c) S. Grimme, *Chem. Eur. J.* **2012**, *18*, 9955 – 9964; d) S. Grimme, M. Steinmetz, *Phys. Chem. Chem. Phys.* **2013**, *15*, 16031 – 16042; e) T. Risthaus, S. Grimme, *J. Chem. Theory Comput.* **2013**, *9*, 1580 – 1591.

[10] G. Giordano, R. H. Crabtree, *Inorg. Synth.* **1990**, *28*, 88 – 90.

[11] E. W. Abel, M. A. Bennett, G. Wilkinson, *J. Chem. Soc. A* **1959**, 3178 – 3182.

[12] D. Hanh Nguyen, N. Lassauque, L. Vendier, S. Mallet-Ladeira, C. Le Berre, P. Serp, P. Kalck, *Eur. J. Inorg. Chem.* **2014**, 326 – 336.

[13] a) A. Ceccon, A. Gambaro, S. Santi, G. Valle, A. Venzo, *J. Chem. Soc. Chem. Commun.* **1989**, 51 – 53; b) C. Bonifaci, A. Ceccon, A. Gambaro, P. Ganis, S. Santi, G. Valle, A. Venzo, *Organometallics* **1993**, *12*, 4211 – 4214; c) A. Ceccon, C. J. Elsevier, J. M. Ernsting, A. Gambaro, S. Santi, A. Venzo, *Inorg. Chim. Acta* **1993**, *204*, 15 – 26; d) C. Bonifaci, A. Ceccon, A. Gambaro, P. Ganis, S. Santi, A. Venzo, *Organometallics* **1995**, *14*, 2430 – 2434; e) C. Bonifaci, A. Ceccon, S. Santi, C. Mealli, R. W. Zoellner, *Inorg. Chim. Acta* **1995**, *240*, 541 – 549; f) C. Bonifaci, A. Ceccon, A. Gambaro, P. Ganis, S. Santi, G. Valle, A. Venzo, *J. Organomet. Chem.* **1995**, *492*, 35 – 39.

[14] T. Schwabe, S. Grimme, J.-P. Djukic, *J. Am. Chem. Soc.* **2009**, *131*, 14156 – 14157.

[15] F. Weinhold, C. R. Landis, *Valency and Bonding, a natural bond orbital donor-acceptor perspective*, University Press, Cambridge, **2005**.

[16] J. Tao, J. P. Perdew, V. N. Staroverov, G. E. Scuseria, *Phys. Rev. Lett.* **2003**, *91*, 146401.

[17] A. Ceccon, A. Gambaro, A. Venzo, V. Lucchini, T. E. Bitterwolf, J. Shade, *J. Organomet. Chem.* **1988**, *349*, 315 – 322.

[18] A. Bondi, *J. Phys. Chem.* **1964**, *68*, 441 – 451.

[19] a) J. Contreras-García, E. R. Johnson, S. Keinan, R. Chaudret, J. P. Piquemal, D. N. Beratan, W. Yang, *J. Chem. Theory Comput.* **2011**, *7*, 625 – 632; b) E. Johnson, S. Keinan, P. Mori-Sanchez, J. Contreras-Garcia, A. J. Cohen, W. Yang, *J. Am. Chem. Soc.* **2010**, *132*, 6498 – 6506.

[20] a) R. F. W. Bader, *Atoms in Molecules*: *A Quantum Theory*, Clarendon, Oxford, **1990**; b) P. Popelier, *Atoms in Molecules*, *An Introduction*, Prentice Hall, Harlow, England, **2000**.

[21] K. B. Wiberg, *Tetrahedron Lett.* **1968**, *24*, 1083 – 1096.

[22] a) M. P. Mitoraj, A. Michalak, T. Ziegler, *Organometallics* **2009**, *28*, 3727 – 3733; b) M. P. Mitoraj, A. Michalak, T. Ziegler, *J. Chem. Theory Comput.* **2009**, *5*, 962 – 975.

